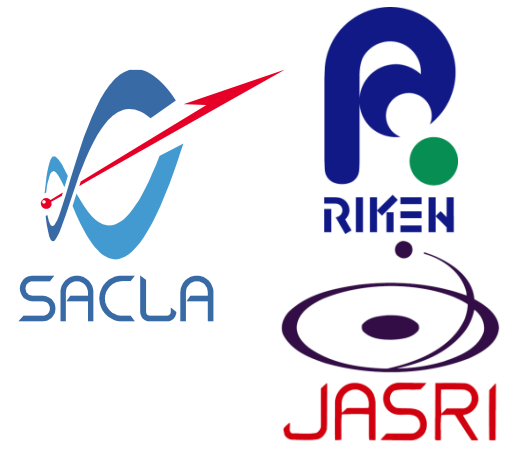


# Indirect X-ray imaging detector resolving 200 nm line-and-space patterns by using composite of transparent ceramics

SACLA Users' Meeting 2019 poster No. 10

Takashi Kameshima<sup>a, b</sup>, Akihisa Takeuchi<sup>a</sup>, Kentaro Uesugi<sup>a</sup>, Togo Kudo<sup>a, b</sup>, Yoshiki Kohmura<sup>a, b</sup>, Kenji Tamasaku<sup>a, b</sup>, Makina Yabashi<sup>a, b</sup> and Takaki Hatsui<sup>a, b</sup>



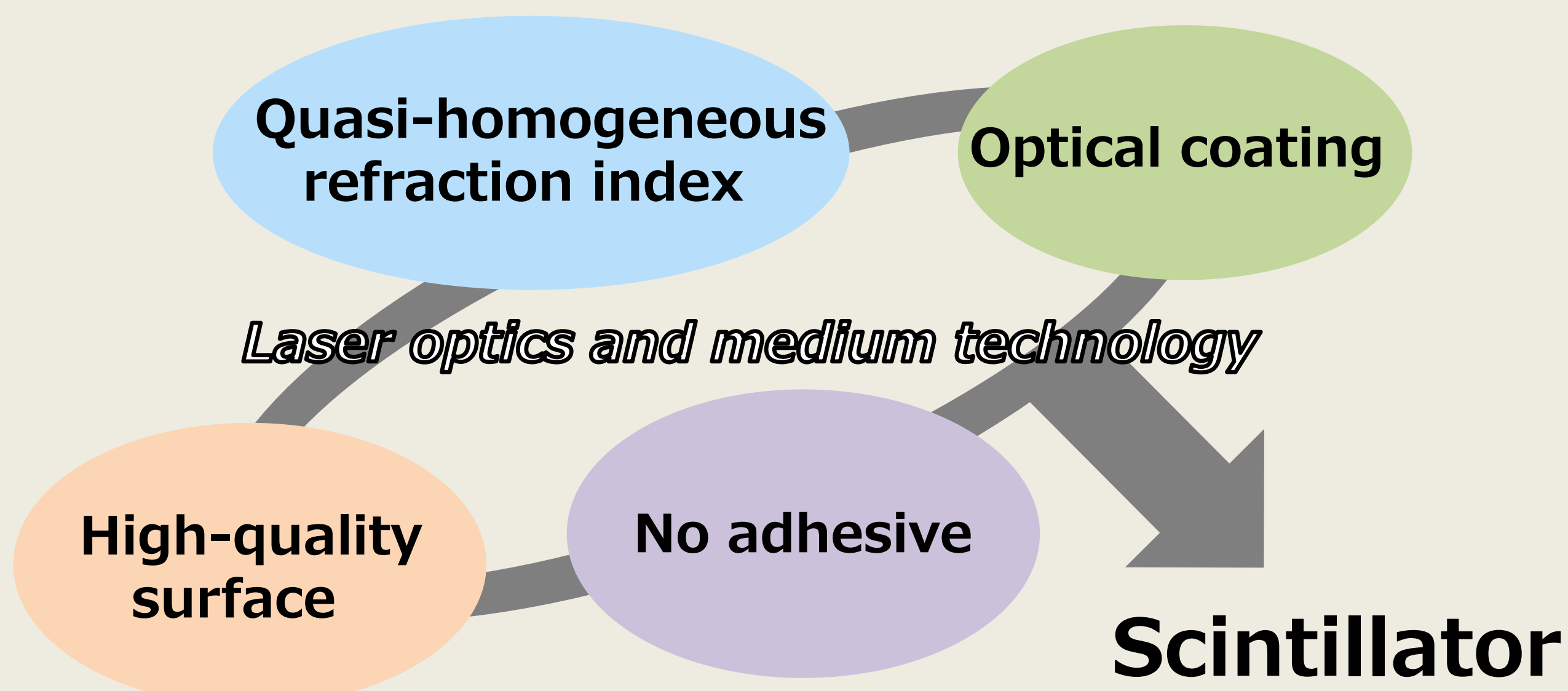
<sup>a</sup>Japan Synchrotron Radiation Research Institute, <sup>b</sup>RIKEN SPring-8 center  
Email: kameshima@spring8.or.jp

## Abstract

A high-resolution lens-coupled X-ray imaging detector equipped with a thin-layer transparent ceramics scintillator has been developed. The scintillator consists of a 5  $\mu\text{m}$ -thick Ce doped  $\text{Lu}_3\text{Al}_5\text{O}_{12}$  layer (Ce:LuAG) bonded onto the support substrate of the non-doped LuAG ceramics by using a solid-state diffusion technique. The effective pixel size on scintillator plane was 65 nm. X-ray transmission images of 200 nm line-and-space patterns were successfully resolved. X-ray imaging of very large scale integration (VLSI) circuits was demonstrated and the wiring patterns in the inner layers were clearly visualized.

## Introduction

We applied high power laser optics and medium technology [1,2] to a scintillator. This provides quasi-homogeneous refraction index structure, high-quality surface, direct bonding without adhesive layer, and optical coating.



- **Elimination of optical problems such as**
  - ✓ Defocus light
  - ✓ Light diffusion ( multi-reflection, scattering )
  - ✓ Wave front aberration
- **Direct bonding**
  - ✓ provides radiation hardness because of no-adhesive layer
- **Radiation shield**
  - ✓ Millimeter-thick substrate attenuates X-ray to  $10^{-43}$  order at 10 keV. This enables high NA lens with short working distance to be installed.

## Fabrication process of a thin film scintillator

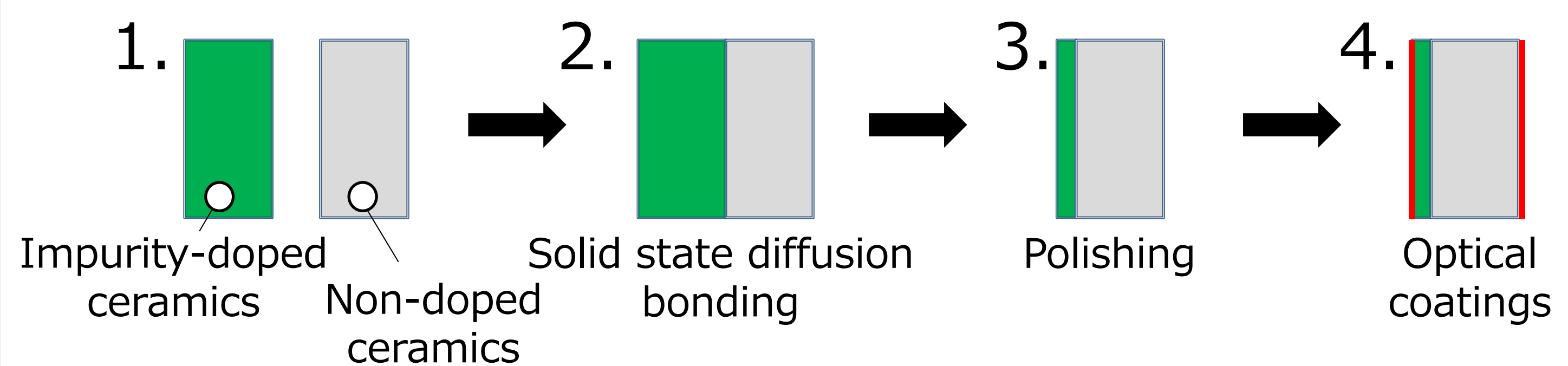


Fig. 1 Schematic of a thin-film scintillator layer fabrication [3]

1. A scintillator and a substrate are produced from identical material.
2. The composite of the impurity-doped ceramics (scintillator) and the non-doped ceramics (substrate) are formed by the solid-state-diffusion bonding method.
3. The scintillator layer is grinded, lapped and polished to be thinned down to  $\sim 5 \mu\text{m}$ .
4. The surface of non-doped ceramics is coated by an anti-reflection film. For the surface of impurity-doped ceramics, there are two options of anti-reflection or reflection films.

## Produced scintillators

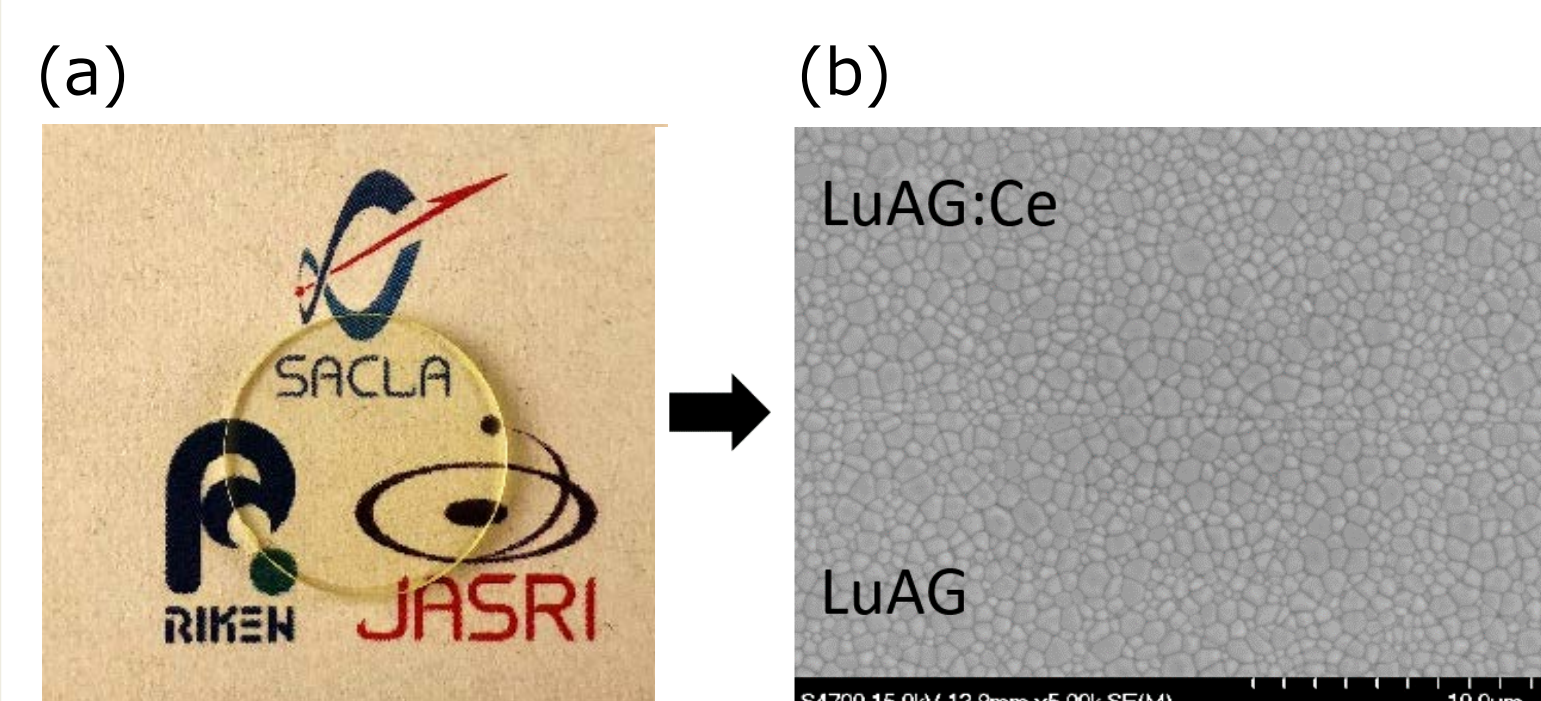


Fig. 2 (a) Photograph of 5  $\mu\text{m}$  thick LuAG:Ce on 1 mm thick LuAG  
(b) Secondary electron micrograph of bonded interface of LuAG:Ce and LuAG

The scintillator thickness can be controlled in wide range scale of  $\mu\text{m} \sim \text{mm}$  order. The production of a large scintillator with an area of up to 100 mm is also available by using solid-state-diffusion bonding method. The transparent ceramics and solid-state-diffusion bonding technique are provided by Konoshima Chemical Co.,Ltd [1, 2].

## Evaluation results

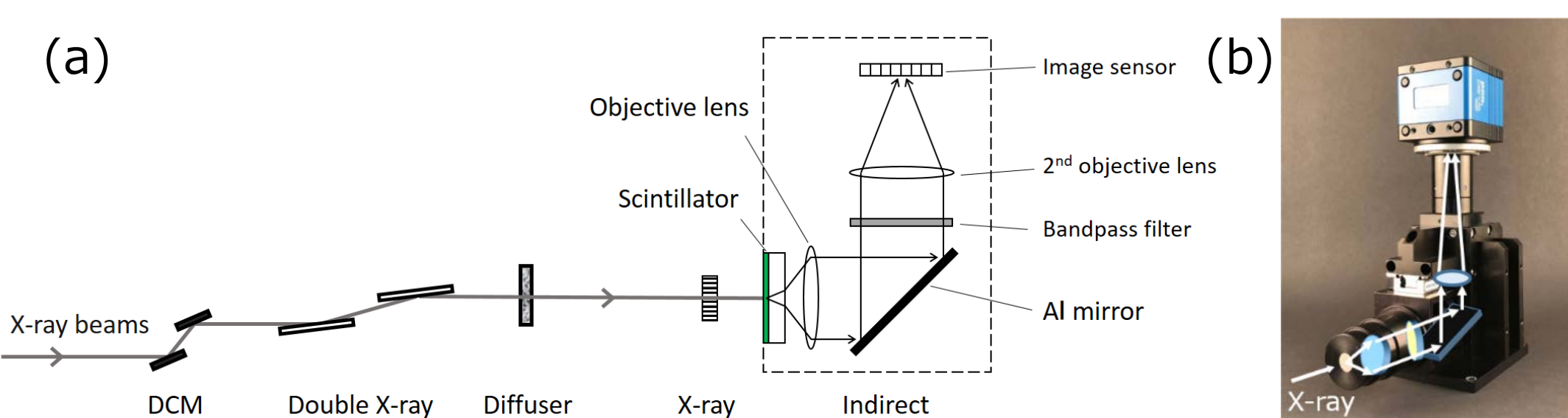


Fig. 3 (a) Experimental setup  
(b) Photograph of X-ray imaging detector

- SPring-8 BL29XU collimated X-ray beam (unity magnification)
- 5  $\mu\text{m}$ -thick Ce:LuAG (520 nm fluorescence)
- Numerical Aperture: 0.85
- Effective pixel size: 65 nm
- Working distance  $\sim 0.5 \text{ mm}$  to minimize X-ray diffraction

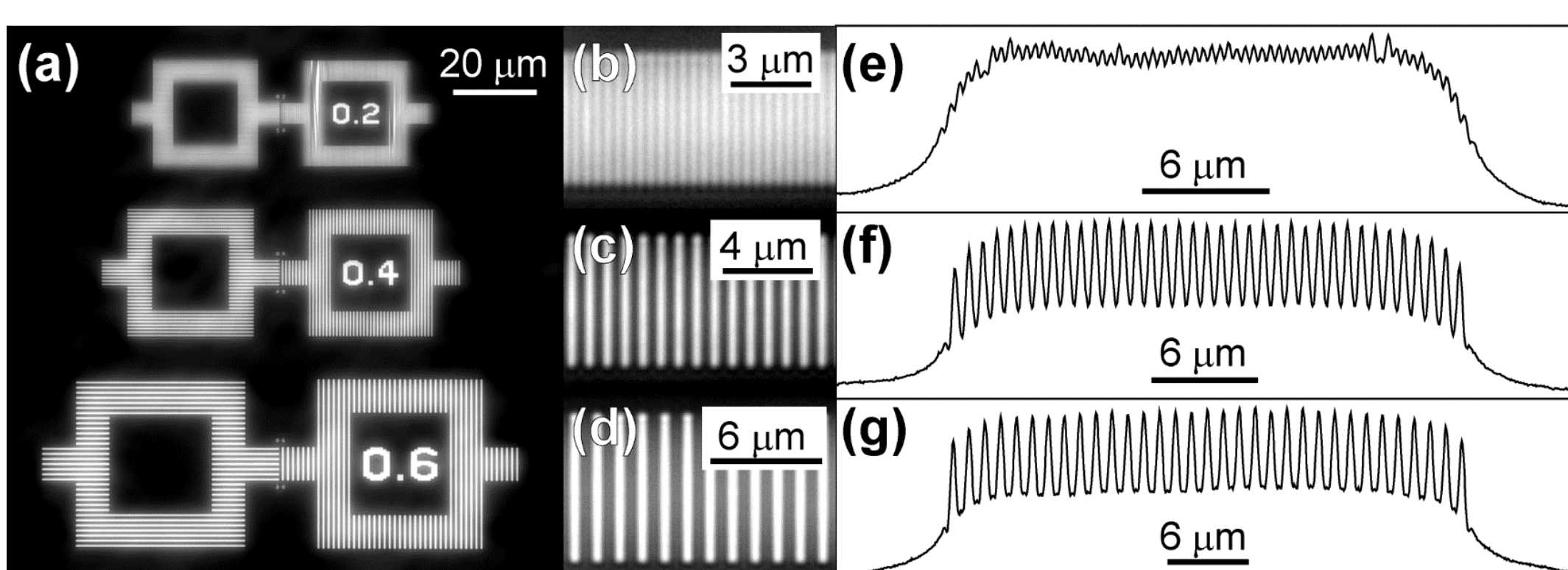


Fig. 4 (a) Microradiograph of tantalum line-and-space patterns at photon energy of 7.3 keV.  
(b, c, d) Zoomed images at the area of 200, 400, and 600 nm line-and-space patterns, respectively.  
(e, f, g) Projection profiles at the areas of 200, 400, 600 nm line-and-space patterns, respectively.

- 200 nm line-and-space was clearly resolved.
- The contrast of 400 nm and 600 nm patterns have achieved to nearly 50 %

- Cutoff frequencies have achieved 2500 lines/mm or higher at every photon energy of 7.3  $\sim$  18 keV

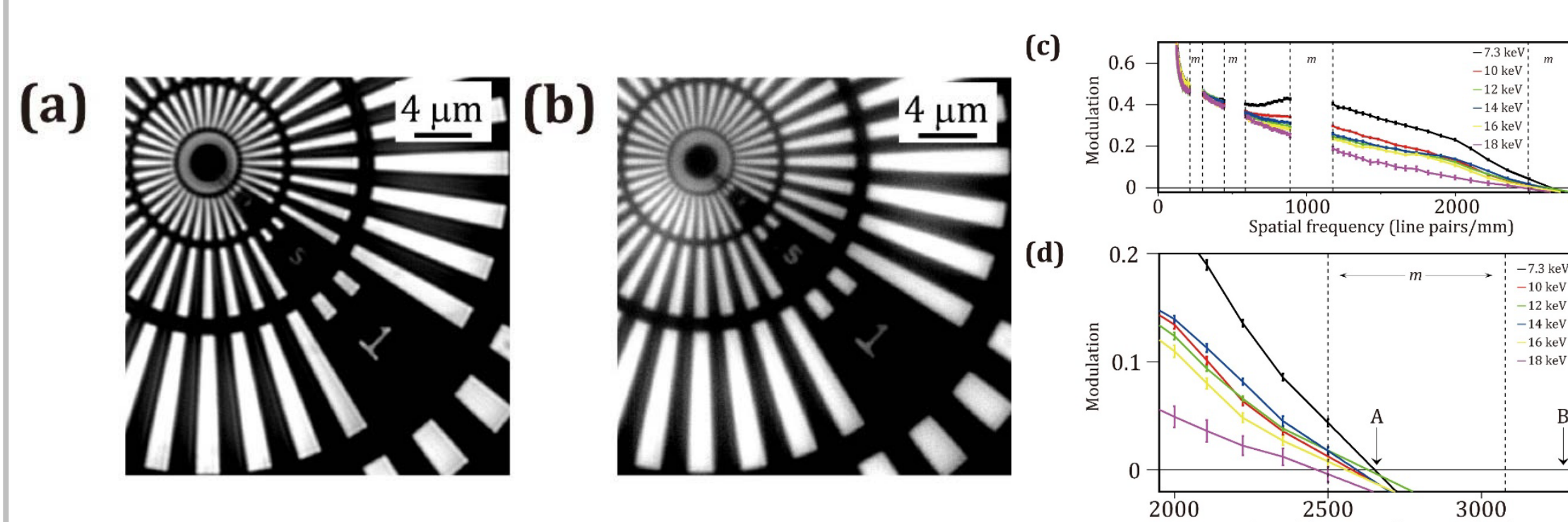


Fig. 5 (a, b) X-ray transmission image of the Siemens pattern at 7.3, 16 keV. (c) Plot of modulation transfer function at photon energy of 7.3  $\sim$  18 keV. (d) zoom of (c) at cutoff frequency region

The detector has successfully resolved 200 nm line-and-space patterns. The diffraction limit for the fluorescence wavelength of 520 nm and  $\text{NA} = 0.85$  gives 153 nm cutoff line width. The cutoff line width 189 nm at 7.3 keV is comparable to the diffraction-limit performance [4].

## X-ray imaging of a Very-Large-Scale-Integration (VLSI) chip

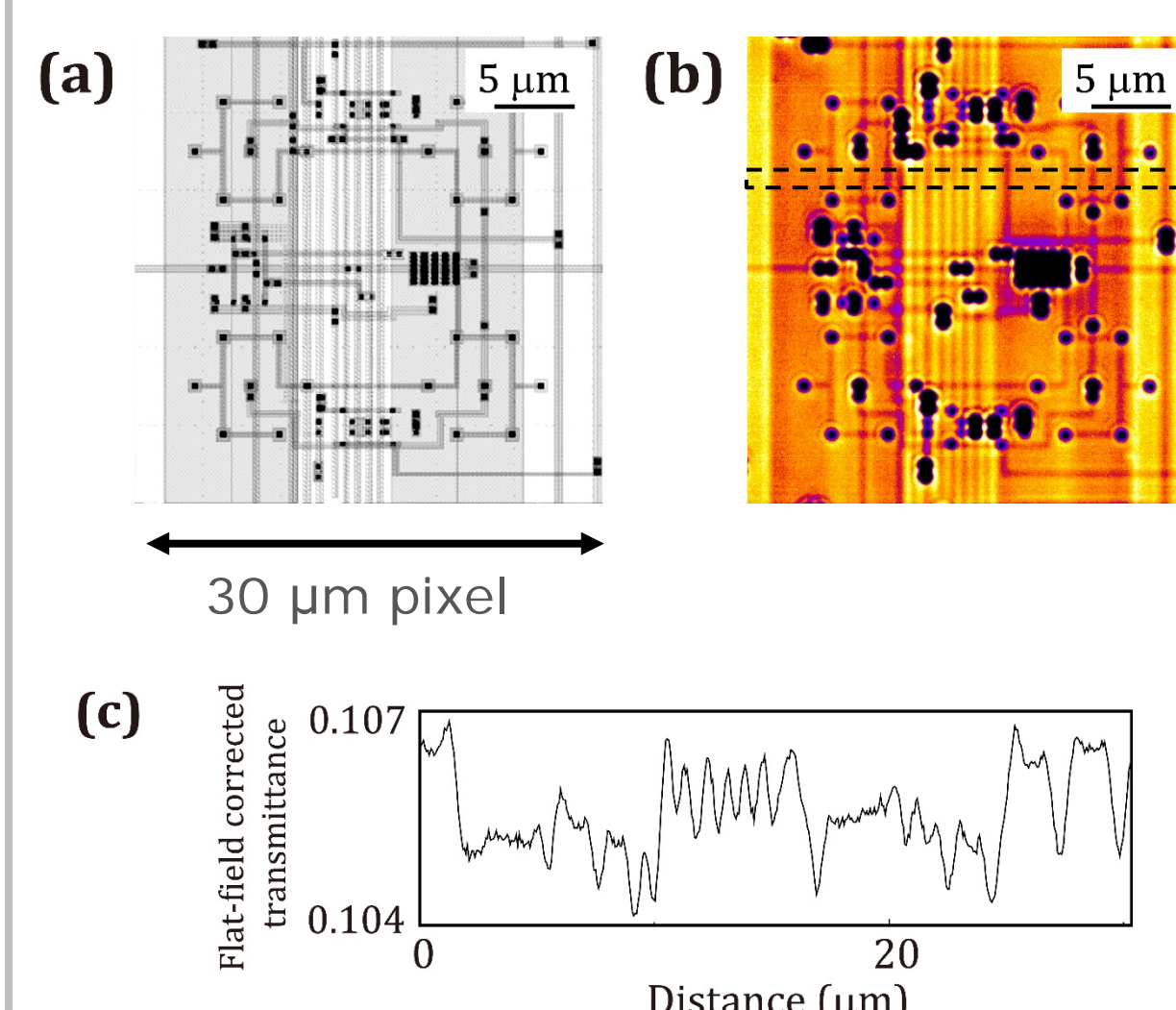


Fig. 6 (a) Circuit design drawing of metal layers in the 3 x 3 SOPHIAS imaging pixels  
(b) X-ray transmission image acquired by the developed detector  
(c) Line profile calculated for the image section depicted as a dotted rectangle in (b)

- Sample: SOPHIAS chip
- Aluminum lines had a minimum width of 300 nm and 600 nm thickness.
- Silicon chip has 500  $\mu\text{m}$  thickness. This is significantly thicker than aluminum wire lines.
- The present detector successfully visualized these low contrast and deep sub-micrometer patterns [4].

## Upgrade plan 1 ( enhancement of FOV )

We are planning to employ a large format CMOS image sensor and develop the dedicated objective lens.

	Present system	Upgrade system
Resolving power	200 nm line & space	250 nm line & space
FOV	133 x 133 $\mu\text{m}^2$	2,500 x 1,900 $\mu\text{m}^2$
Image format	2048 x 2048, 65 nm pixels	14,192 x 10,640, 177 nm pixels

## Upgrade plan 2 ( enhancement of spatial resolution )

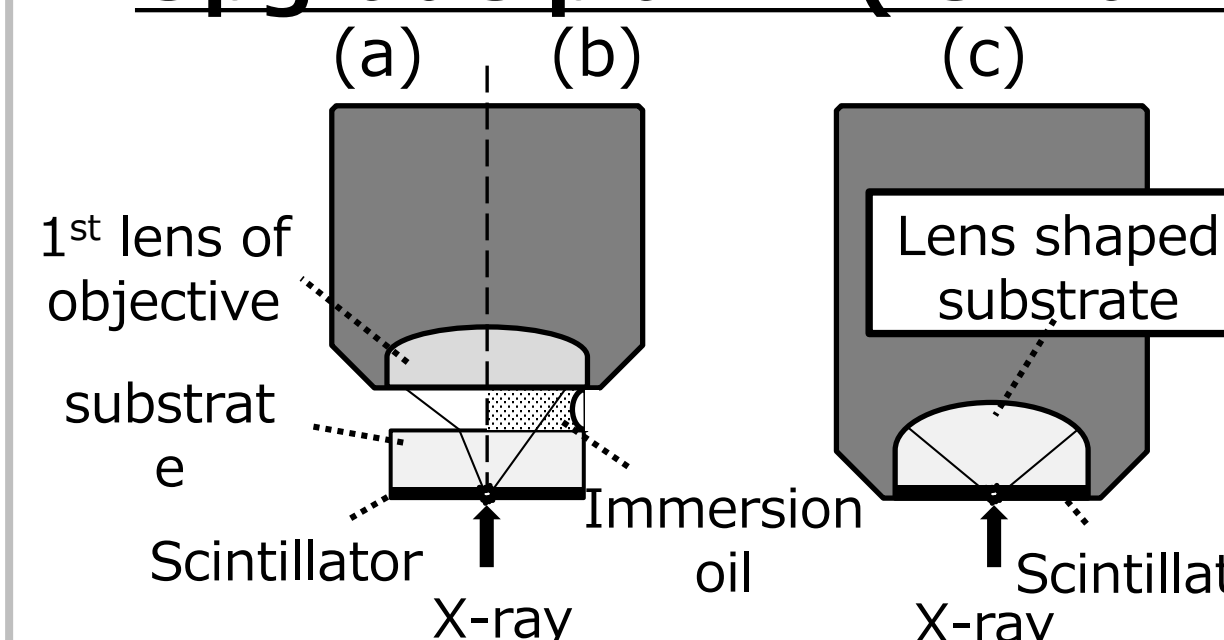


Fig. 7 Comparison of the objective lens structure.  
(a) dry lens. (b) liquid immersion lens. (c) solid immersion lens

We are planning to develop a solid immersion lens with super high NA 1.54 by installing the lens-shaped scintillator substrate as first lens. This optical design is capable of achieving sub-100 nm line & space visualization.

## Summary

The developed indirect detector has successfully resolved 200 nm line-and-space patterns. This resolving power has successfully visualized wiring patterns and vias in the VLSI circuit.

## References

- [1] H. Yagi et al., Opt. Mater. 29 (10), 1258 (2007).
- [2] H. Yagi, Jpn. J. Appl. Phys. 45 (2L), L207 (2006).
- [3] T. Kameshima et al., AIP Conf. Proc. 1741, 040033 (2016).
- [4] T. Kameshima et al., Optics Letters 44, 1403 (2019)